ISSN 0915-633X

NATIONAL INSTITUTE FOR FUSION SCIENCE

New Method of Error Elimination in Potential Profile Measurement of Tokamak Plasmas by High Voltage Heavy Ion Beam Probes

Y. Hamada, K. Masai, Y. Kawasumi, H. Iguchi, A. Fujisawa and JIPP T-IIU group

(Received – Feb. 5, 1992)

NIFS-143 Apr. 1992

RESEARCH REPORT
NIFS Series

NAGOYA, JAPAN

New Method of Error Elimination in Potential Profile Measurement of Tokamak Plasmas by High Voltage Heavy Ion Beam Probes

Y. Hamada, K. Masai, Y. Kawasumi, H. Iguchi, A. Fujisawa
and JIPP T-11U group

National Institute for Fusion Science
Nagoya, 464-01, Japan

ABSTRACT The measurement of a potential profile in tokamak plasmas by heavy ion beam probe(HIBP) in a single shot is usually difficult, because as primary beam is swept through plasma cross-section, the secondary beam hits the input slit of an energy analyzer with a large variation in entrance angles(in-plane and out-of-plane). In this paper, a new method(the application of fast toroidal sweeps of the primary or the secondary beam at the analyzer or at an entrance to an tokamak) is proposed to eliminate the error due to the change in the entrance angle. In addition, results of a new calibration method of HIBP in tokamaks(electron stripping by neutral gas) are presented.

Keywords, HIBP, tokamak, potential, analyzer, beam.

§1 Introduction

The heavy ion beam probe(HIBP) in a magnetic confinement system is particularly useful for the measurement of local electric potential and fluctuations of local plasma density and potential[1]. The first precise measurement of a potential profile of the tokamak plasma, was performed in ST tokamak[2]. But its measurement was conducted at a very low current of about 20kA where the deviation of the secondary beam from one poloidal plane was very small. It means that trajectories of the beam in the analyzer stay nearly in the analyzer plane(plane of symmetry of the

analyzer and perpendicular to the plane of analyzer electrode) because of small deflection due to plasma current. In this case, the error in the measurement of total energy of the beam is insignificant, since beam velocity perpendicular to the analyzer plane, is small. In ISX-B tokamak, potential profiles of ohmic plasmas and those of plasmas with co and counter neutral beam injection, were measured by shot-to-shot basis[3] in order to eliminate the error due to the change in entrance angles, caused by the scanning of plasma cross-section. Similar measurements were performed in TM-4 and TEXT tokamaks[4,5].

The reason for the change in an in-plane entrance angle to an analyzer is illustrated in Fig 1a. The secondary beam generated in different places in the plasma, has a shape similar to a sheet. The small portion of the sheet, generated at a certain point in the plasma, goes through the input slit of the analyzer and hits the detector. If we sweep an injection angle of the beam at an entrance to the tokamak, we can observe beams generated in different places in the plasma, but the secondary beam goes through the slit with different entrance angles to the analyzer as shown in Fig. 1a.

As for an out-of-plane entrance angle, let's consider a case of the injection of heavy-ion probing beam into an axisymmetric confinement system, for simplicity. Because of a change in charge state, the secondary beam carries the information of a local plasma potential and a local stream function, where it is ionized, as shown in Fig.1b, through the conservation of energy and canonical angular momentum. When the probing beam is initially injected perpendicularly to the toroidal field and the local value of the stream function at the analyzer is the same with that of the stream function at the injection point because those points are far away from the plasma, the changes in beam energy (ΔE) and angular momentum ($mrv_\phi + erA_\phi$) are simplified and given by

$$\Delta E = e(\Phi(\bar{r}_X) - \Phi(\bar{r}_{analyzer})), \quad (1)$$

$$mrv_{\phi,analyzer} = e(\Psi(\bar{r}_X) - \Psi(\bar{r}_{analyzer})), \quad (2)$$

where, r_X is the position where ionization of the primary beam by the plasma occurs. $\Psi(r)$ is a stream function(rA_ϕ) and $\Phi(r)$ is an electric potential. Since $v_\phi/(v_r^2+v_\phi^2)^{0.5} - \Omega$, is an out-of-plane injection angle to the analyzer where Ω is an angle between the analyzer plane and the injection plane of the beam, the change in the out-of-plane entrance angle during scanning of plasma cross-section is inevitable and is significant when plasma current is large.

The error due to the change in an in-plane entrance angle to an analyzer, can be suppressed significantly if we use an analyzer with focusing up to the second order. Up to now, for scanning plasma cross-section by HIBP, we have to tune shot by shot, the direction of the analyzer so that an out-of-plane entrance angle should be zero, at each spatial point of the measurement for the suppression of the error. In order to get a precise profile of plasma potential, we have to invent a new method to eliminate the error instead of relying on shot by shot measurements.

Recently energy of the beam for HIBP in tokamaks has been increased to 0.5MeV in TEXT[7] and JIPP T-11U tokamaks[8] and the development of a new 2MeV HIBP for TEXT is under way[13]. The energy of the injected beam itself has the stability of the ripple less than a few volts out of 500kV in JIPP T-11U HIBP, since the HIBP usually utilizes a thermionic ion gun[6] and a highly stabilized high voltage power supply. Accordingly, the error in a potential measurement by HIBP may be determined by the error in an energy analyzer. Since the error due to the energy analyzer is proportional to the beam energy, a new method for the calibration and elimination of the error in an energy analyzer is urgently needed.

The calibration and the check of the alignment of HIBP system is so far done by an introduction of a primary beam to an energy analyzer of the HIBP. The disadvantage of the calibration and the check of the alignment using the primary beam is that basic parameters of the tokamak and HIBP, such as toroidal field, beam voltage, analyzer voltage and the trajectory to the analyzer, under which the primary beam is injected into the vacuum vessel and guided into the energy analyzer, are entirely different from those under which the secondary beam generated in the vacuum vessel is guided into the analyzer. Accordingly, the calibration of the system is done with many assumptions, the linearity of the voltage of the analyzer and, exact adjustment to changes in both in-plane and out-of-plane entrance angles to the analyzer. A very reliable calibration in the routine measurement is almost impossible.

Another error in a measurement of plasma potentials is caused by difficulties of very accurate measurements of the absolute value of an accelerating voltage of the beam(about 500kV) and an analyzer voltage(100kV) for the calibration of the absolute measurement of the plasma potential. The relative change of the potentials has been measured up to now. Accordingly, a new systematic way of the calibration of zero potential during scanning of plasma cross-section is also required.

Recently at ATF HIBP experiment, gas ionization of the beam is employed for the calibration of zero potential[14]. It is a great improvement of HIBP in the toroidal machine. It is particularly suited to helical machines, where the beam trajectory does not change appreciably by the presence of the lowβ plasma. But as for a tokamak, the secondary beam due to gas ionization has not been detected since the analyzer is adjusted to the beam with large deflection in the toroidal direction.

Here we are going to discuss the first experiment of a calibration of HIBP by neutral gas and a new idea of fast

beam sweeping for the error elimination in a potential profile measurement of tokamak discharges.

$ 2 Error Analysis in the Measurement

Figure 2 shows the total arrangement of HIBP system in JIPP T-11U[8]. The heavy ion beam from a 500keV electrostatic accelerator is guided by an electrostatic deflector into the tokamak. Two quadrupole electrostatic lenses are installed for beam transport and focusing in the center of tokamak plasmas. At the entrance to the tokamak, toroidal and poloidal sweepers are installed. A poloidal sweeper is used to scan plasma cross-section. A toroidal sweeper is used to compensate the beam displacement in the toroidal direction at an analyzer, which is induced by plasma current. The analyzer used here is a parallel plate electrostatic analyzer with entrance angle of 30 degrees and focusing up to the second order.[9]

Figure 3a shows a cross-sectional view of trajectories, of primary beams and the secondary beam generated in the plasma during scanning of plasma cross-sections by sweeping the injected beam. The modelling of the toroidal coil must be accurate, since the ripple of the toroidal field affects the beam trajectory significantly. Poloidal fields are calculated using plasma equilibrium code with real poloidal coil parameters.

The secondary ions produced on the dotted line in Fig. 3a are allowed to enter the input slit of the energy analyzer. Accordingly, along the dotted lines, a potential profile is measured through a sweep of the beam at the entrance into the tokamak. Inevitably, an entrance angle(in-plane) to the analyzer changes noticeably by the sweep of the beam for the scanning of plasma cross-section. Figure 3b shows a plane view (x,y coordinates, if the symmetry axis of tokamak is taken to be z axis) of trajectories with the same parameters in Fig 3a.

It is clearly shown that during scanning of the cross-section, an out-of-plane injection angle as well as a

horizontal place on the input slit of the analyzer, changes appreciably. In addition, the breaking of the conservation of canonical angular momentum is clearly observed by behaviours of the primary beam in the region far from the plasma. When axisymmetric toroidal coil is assumed in the calculation, trajectories of the primary beam are lines intersecting the axis of symmetry in Figure 3b in the field free region, since the initial injection is radial(v_ϕ=0) as is observed in Figure 3b. In the real case, the ripple of the toroidal field affects the radially injected beam significantly and straight lines of trajectories far from the plasma do not intersect the axis of symmetry as shown in Figure 3b.

There are two types of electrostatic analyzers which have good focusing up to the second order, a plane mirror energy analyzer(parallel plate analyzer) and a cylindrical mirror energy analyzer[12] . Because of a large shift of the entrance point on the input slit in the horizontal direction, the cylindrical mirror analyzer is not used, although the error due to the out-of-plane entrance angle does not exist in it. By this reason, the energy analyzer commonly used in HIBP is a parallel plate electrostatic analyzer with 30 degree injection angle.

The plasma potentials($\Phi(r_x)$) are reduced from the beam energy(V_b) and the analyzer voltage(V_a) by the following equations[10]

$$\Phi_p(r_x) = V_b - V_a(q_s - q_p)G(\theta)(\cos\varphi_b)^{-2} \quad , \qquad (3)$$

where θ, φ_b are in-plane and out-of-plane entrance angles. q_s and q_p are charge numbers of the secondary and primary beams respectively. The gain function $G(\theta)$ is the main characteristics of the analyzer and is the ratio of the beam energy in the analyzer plane to an analyzer voltage when the beam is in the middle of the upper and lower detector plates. It is theoretically given by

$$G(\theta)=\frac{q_b}{2Hl}\,\frac{L_t-(h_i+h_d)\cot\theta}{\sin 2\theta}, \qquad (4)$$

where L_t is the distance between the slit and the detector, and h_d and h_i are distances between the parallel plate and the detector or the slit respectively. Hl is a distance between upper and lower electrode as is shown in Figure 1a. The $G(\theta)$ must be determined experimentally, since the theoretical estimate(4) is a little different from the experimental value because the accuracy of the physical size of the analyzer, the separation of the parallel electrodes for example, may not exceed 10^{-4}, while the accuracy of the $G(\theta)$ is required up to 10^{-4} or more.

The error due to the change in in-plane and out-of-plane entrance angles is obtained by equation(4) and (3) and is given as follows,

$$\Delta\Phi_p(\bar{r})\approx -V_b\varphi_b{}^2+32V_b(\Delta\theta)^3, \qquad (5)$$

where $\Delta\theta$ is the deviation of θ from the second order focus angle of 30 degrees.

As is shown in Fig. 3b, the v_ϕ/v_b can be about 0.1. The error due to the out-of-plane entrance angle is comparable to or larger than an expected plasma potential of a few kV in the tokamak when the 500keV beam is used, if an analyzer is set parallel to the injection plane into the tokamak. In addition, the error due to the deviation of in-plane angle from 30 degrees also becomes significant when the deviation is not small, because of the cubic power of $\Delta\theta$ and the large coefficient of 32. Accordingly, at each measurement of one spatial point, the energy analyzer has been adjusted in two directions, so as to keep an in-plane entrance angle to be 30 degrees and an out-of-plane entrance angle to be zero.

§3 Calibration by Neutral Gas

The other error in the measurement of plasma potentials is caused by difficulties of the accurate measurement of the absolute value of the very high accelerating voltage of the beam(about 500kV) and the analyzer voltage(about 100kV) in the equation(3). These difficulties cause uncertainties in the experimental determination of zero potential and the gain factor of the analyzer in a very high voltage region. In order to suppress these errors, a calibration of the total HIBP system by the electron stripping by neutral gas is adopted. The cross-section $\sigma_{1,2}$ of electron stripping for Tl^{1+} or Cs^{1+} ion in the gas,

$$Tl^{1+} + H_2 = Tl^{2+} + H_2 + e,$$

grows significantly in the energy range from 200keV to 500keV as shown in Table 1[15]. This means that as for the generation of the secondary beam, the neutral gas behaves similarly to the plasma.

The check of the alignment and calibration by neutral particles is particularly useful, since the almost entire condition is the same with the plasma experiment except the difference in the plasma current. Also the energy loss of the beam by the gas ionization can be estimated to be less than a few volts. In addition, in tokamaks, motions of the beam injected nearly perpendicularly to the tokamak, in the x,z plane in Fig. 3, are mainly determined by the strongest field of toroidal field. The trajectories of those beams are almost same each other, as long as v_ϕ / v_b is small. This means that the in-plane entrance angle to the analyzer is almost the same with one without the plasma current even in case of large plasma current. Accordingly, the error due to the change in an in-plane entrance angle during scanning of the plasma cross-section, can be detected by the gas ionization method as a shift of zero potential, and can be compensated. Accordingly, the calibration by neutral gas can be an important way of zero potential

calibration for HIBP. The error due to an out-of-plane entrance angle can be compensated by our new idea and is discussed in the next section.

Figure 4a shows signals of the secondary beam in the analyzer. This is the first observation of the secondary beam generated by neutral gas in the tokamak since, in the usual measurement, the energy analyzer is stationed with an angle of a few degrees to the X-axis to detect the deflected beam by plasma current. In that case it is impossible to detect the secondary beam due to gas ionization which has no toroidal deflection, unless the detector plate is long enough to cover the beam without deflection, as is shown in Fig 3(b). D_2 gas is introduced into the vacuum vessel through a fast valve. Cross-sections of ionization or recombination of Tl in D_2 and H_2 are considered to be nearly equal because the mass number of Tl is much larger than those of D_2 and H_2. The injected Tl^+ current into the tokamak is a few μA. Since the shape of the secondary beam, generated by neutral gas in the vacuum vessel, is similar to a sheet or a curtain, as is discussed in the case of the plasma, we can observe the secondary ions, in the different places such as the input slit which is composed of split plates, electrically insulated each other , and pair plates of the detector. In Fig.4a, the structure of the split-input-slit is shown. The beam is swept toroidally in order to measure the beam size at the slit. Fig.4b, the expanded view of the traces of Fig.4a, clearly shows that the beam size at the analyzer is much less than the horizontal opening of the slit(4cm) of the analyzer and the signal at the detector is not intercepted horizontally by the input slit.

The detected signals at the split slit and the signals at the detectors of the analyzer show different characteristics in time behaviors. Gas pressure starts to rise linearly after the opening of the gas valve and reaches the value of 1.2×10^{-3} torr at 50msec after the opening. After 120 msec when the valve is closed, the gas pressure decays slowly, because the pumping time constant

of the tokamak is about 1 second. The signals of the currents of the split entrance slit are roughly proportional to the gas pressure of the tokamak. Although the primary beam can not arrive at the analyzer slit without any ionization by neutral gas, as is shown in Figure 3a, currents on the split slit can be a mixture of singly ionized(recombined from doubly ionized beam) and doubly ionized beams. Schematics of the trajectories of singly ionized beam on the analyzer slit are shown in Figure 5a. The currents of the detector in Fig 4a should be doubly ionized beam because the voltage of the analyzer is tuned to doubly ionized ions.

The decrease in signals at the detectors, while the current on the slits is still increasing, may be due to the recombination of doubly ionized ions, electron capture,

$$Tl^{2+} + H_2 = Tl^{1+} + H_2^{1+}$$

The difference in time behaviours is also explained by the fact that the recombination of doubly ionized beam may reduce its contribution to the current on the slit roughly to half, because the recombined singly ionized beam has a shape of a sheet and some part of the sheet can go through the slit. On the contrary, the recombined singly ionized beam can not hit the detector because the analyzer is tuned to doubly ionized particles.

Although the cross-section of the recombination of doubly ionized thallium in the gas, $\sigma_{2,1}$, is not measured[15], the reasonable estimation is that $\sigma_{2,1}$ is a little larger than $\sigma_{1,0}$. At 40 msec after the start of gas puff, the currents on the detector begin to decrease. At this time, the mean free path for $\sigma_{1,0}$ is about 5 meters and is comparable to the experimental dimensions. So it is a reasonable assumption that the recombination of the secondary beam is the reason for the decrease in the detector current. This can also explain the temporal shift of the peak current in the detector at different gas puffing rates as shown in Figure 4c. The peak of the

detector signal occurs at the time when the pressure inside the vessel is roughly the same. Since the signals at the detector are determined by the competition of the ionizing process of the primary beam and the recombination of the doubly ionized beam, the pressure at the peak must be equal and should be dependent only on geometric configuration.

As is mentioned, the time behavior of the signals is explained roughly by the attenuation of the secondary beam. As for quantitative analysis, Monte Carlo analysis of the trajectory to describe effects of the change of state, must be performed to understand fully signals on the input slit. In this calculation, the expansion of the gas into the sweepers, deflectors and lense system, must be taken into consideration.

The currents on the detector plates, even tuned to doubly ionized beams, are affected by complex changes of charge state on trajectories. Some examples of changes are shown in Figure 5b. One is recombination of singly ionized particles and its subsequent ionization in gas. Because of this effect, the injected primary beam itself forms a current sheet as shown in Figure 5b. The other is recombination and its subsequent ionization of the secondary beam as shown in Fig.5b. The effects due to these multiple processes are the broadening of entrance angles(in-plane and out-of-plane) and the degradation of spatial resolution of the measurement. For the quantitative analysis of this effect, Monte Carlo analysis is necessary. In the limit of low gas puffing, however, heavy ions on the detector are only due to single ionization of the primary beam and are free from the effect due to multiple ionization and recombination processes. Accordingly, currents on the detector at low gas density limit can be used for the calibration of a zero potential and the effect of the change in an in-plane entrance angle.

$ 4 Elimination of Errors due to the Change of the Out-of-plane Entrance Angle

As is discused, the error due to this change is quite significant in the case of large plasma current. It may be a dominant error when we want to measure the potential profile in a single shot by sweeping the beam through the plasma cross-section. Here we are going to propose a new idea for the automatic elimination of this effect.

We are going to install plates for fast sweeping of the beam in the toroidal direction, in a space between an input slit and a lower parallel plate electrode, where no electric field is applied. The detectors are composed of the 2 long plates(up and down). The change of beam energy is detected by the displacement of the beam in the vertical direction, that means, the ratio of signals of two plates. By the combination of this detector system and the parallel electrode analyzer, the displacement of the beam in the horizontal direction does not induce the error in the measurement.

If we apply high voltage sine wave on the sweep plates inside the analyzer, an out-of-plane angle inside the analyzer changes sinusoidally and it crosses zero at some time during one cycle of the sweep if the sweep angle is larger than the entrance angle induced by plasma current. Only when the beam inside the analyzer is parallel to the analyzer plane, the ratio of the detector signals(up and downs plates) indicates the total energy of the beam, the maximum of the energy corresponding to the motion in the analyzer plane. This maximum energy is free from the error due to an out-of-plane entrance angle.

If we trace local maxima, the error due to the non-zero out-of-plane entrance angle, will be automatically eliminated, although the time response of the total system will be reduced by the introduction of a fast toroidal sweep inside the analyzer. In principle, a change in the energy of the beam induced by a fast sweep can be determined by the ratio of swept time to transit time of the beam in the sweeper and the voltage of the sweepers.

Since the transit time is small because the energy is high and the sweeper is small, it is expected that this method is applicable to about 100kHz.

An alternative method for the compensation of an out-of-plane entrance angle is fast sweeping in the toroidal direction at the entrance into the tokamak. Figure 6 shows contours of ratio of toroidal velocity v_ϕ to the total beam velocity, v_ϕ / v_b as a function of toroidal and poloidal sweep angles at the sweep point at the entrance to the tokamak, as shown in Figure 3a. If we apply a fast sweep in the toroidal direction while we scan plasma cross-section by a slow sweep of a poloidal injection angle as shown in Fig.3a, the out-of-plane angle can be zero at some moment in the fast sweep since v_ϕ / v_b is a smooth and one valued function of the horizontal sweep angle as shown in Fig. 6. At the time $v_\phi / v_b = 0$, the measured energy becomes locally maximum during single fast sweep and is free from the error. The contours in figure 6 are dependent on plasma current, position of the plasma center, current profile, and the beam energy. Accordingly, the exact programmed compensation of out-of-plane angle is difficult and the above mentioned method will be the most basic method. Figure 6 shows also the effect of the ripple of the toroidal field. If we sweep the beam to positive v_ϕ at the entrance to the tokamak, then v_ϕ at the analyzer slit is negative due to the reflection of the beam by the ripple of the toroidal field as shown in Fig.6

The basic disadvantage of this method is to rely on axi-symmetry. If this symmetry is broken, for example due to the drift wave turbulence or so, this method becomes inapplicable. These two methods are, however, independent ways and will form an important cross check for each other.

In these two methods we have to use a fairly wide input slit and detector plates in the horizontal direction in order to have signals due to the gas and plasma ionization at the same shot, since if gas is introduced in the vacuum vessel after the plasma is terminated and if the input slit and detector plates are wide enough, the

calibration can be performed automatically in a single shot. The gain function $G(\theta)$ may change as the horizontal entrance position of the beam on the slit changes, because the horizontal length of the electrodes is finite and there are meshes on the lower electrode to permit the entrance of the beam into the region between upper and lower electrodes. The change of the gain function will cause the error in the measurement of a plasma potential as is shown in equation 3. Accordingly, the design of the analyzer must be carefully performed in order to have the very uniform characteristics on the horizontal entrance position and the calibration of the dependence of the horizontal position becomes essential for a precise measurement of the potential profile. For this purpose, it is very important to have two sweepers in the toroidal direction at the entrance to the tokamak and at the analyzer in the gas calibration experiment. By a sweeper at the entrance to the tokamak, we can sweep a horizontal entrance point of the analyzer and by a fast sweep at the analyzer we can measure the beam energy, eliminating the error dur to the effect of an out-of plane entrance angle. By this method we can measure the dependence of zero potential on the horizontal entrance point, i.e. the calibration of the analyzer with large horizontal opening. In addition, the sensitivity calibration becomes feasible if we slowly change the accelerating voltage.

Since the slit width in the horizontal direction is large, the horizontal sweeper should be an elaborate deflector instead of a parallel plate sweeper. One of appropriate deflectors is an octupole deflector or a higher-order multipole deflector[16] in order to have very low aberrations in a narrow space. A multipole deflector with electrodes on an ellipsoid instead of a conventional circle, is under design. In addition, the modification of the energy analyzer and its access port to the tokamak, is now planned to provide a space for the installation of a deflector at the analyzer.

§5 Summary

Errors in the measurement of a potential profile in the tokamak plasma by a high voltage HIBP are analyzed. For the elimination of the errors, neutral gas calibration and fast sweep methods at the energy analyzer and at the entrance to the tokamak are proposed. The neutral gas calibration method is found to have more complex character compared to the case with plasmas, because recombination cross-section is comparable to or larger than those of ionization of the primary and secondary beams. We have to be careful that the measurement is done at low density limit. Fast sweeping of the beam in the toroidal direction at the entrance to the tokamak and at the energy analyzer is useful, although the time response deteriorates. It may have the frequency limit roughly to 100kHz. In these systems the beam itself crosses the slit at large distance in the horizontal direction and the calibration of the energy analyzer becomes very essential for the elimination of the error. The design of the horizontal sweeper with large horizontal opening width in a narrow space is itself, a challenging task. We started the design of the ellipsoidal multipole deflector. The modification of the analyzer and its access to the tokamak is required in order to have larger space for the installation of the sweepers. The combination of these 2 sweepers will be very powerful for the calibration of the analyzer itself and for obtaining a precise one-shot measurement of a potential profile in the tokamak.

We would like to thank Professors, R. L. Hickok and K. A. Connor of Rensselaer Polytechnic Institute for their kind guidance in the design and construction of HIBP in JIPPT-11U. In addition, the authors acknowledge Director A. Iiyoshi and Professor M. Fujiwara for their continuous supports. The authors express sincere thanks for useful advices in numerical calculation to professors J. Todoroki

and T. Watanabe. Especially the 3-d interpolation program for trajectory calculation is from Prof. T. Watanabe.

Reference

1) J.C.Jobes,and R.L.Hickok, Nuclear Fusion **10** (1970) 195.

2) J.C.Hosea,F,C.Jobes,R.L.Hickok,and A.N.Dellis, Phys.Rev.Letts. **30** (1973)839.

3) G.A.Hallock,J.Mathew,W.C.Jennings,R.L.Hickok, K.A.Conner,A.J.Wooton,and R.C.Isler, Phys.Rev.Lett. **56** (1986)1248.

4) V.I.Bugarya,A.V.Gorshkov,S.A.Grashin,I.V.Ivanov, V.A.Krupin,A.V.Mel'nikov,K.A.Razumova,Yu.A.Sokolov, V.M.Trukhin,A.V.Chankin,P.N.Yushmanov,L.I.Krupnik, I.S.Nedzel'skij, Nuclear Fusion, **12** (1985)1707.

5) X.Z.Yang,B.Z.Zhang,A.J.Wooton,P.M.Schoch,B.Richards, et al., Phys. Fluids, **B3** (1991) 3448.

6) O.Heinz and R.T. Leaves, Rev.Sci.Instrum., **39** (1968) 1229.

7) P.M.Schoch,J.C.Forster,W.C.Jennings, and R.L.Hickok, Rev.Sci.Instrum. **57(8)** (1986)1825.

8) Y.Hamada,Y.Kawasumi,M.Masai, H.Iguchi,A.Fujisawa and JIPP T-11U Group, Annual Review of NIFS (1990) 118.

9) T.S.Green and G.A.Proca, Rev.Sci.Instrum. **41**, (1970)1409.

10) P.M.Schoch,A.Camevali,V.T.P.Crowley,J.C.Forster, R.L.Hickok,J.F.Lewis,and J.G.Schatz,Jr. Rev. Sci. Instrum. **59(8)** (1988)1646.

11) K.Toi,Y.Hamada et al.,in Plasma Physics and Conrolled Nuclear Fusion Research 1990,Vol1,301,IAEA, Vienna (1991).

12) V.V.Zashkvara, M.I.Korsunskii,and O.S.Kormachev, Soviet Physics-Technical Physics **11** (1966)96.

13) P.E.McLaren,K.A.Connor,J.F.Lewis, R.L.Hikok, T.P.Crowley, J.G. Schatz and G.H. Vilardi, Rev. Sci.

Instrum. **61** (1990)2955.
14) K.A.Connor, Private communications.
15) I.Alvarez and C.Cisneros, Phys.Rev.,**13** (1976)1728.
16) E.F.Ritz,JR, Adv. Electron. Electron Phys.,**49** 299 (1979).

Figure Captions

Figure 1

Principles of heavy ion beam probe(HIBP). (a) Schematics of beam trajectories and energy analyzer. (b) Schematics of the change of beam energy on the trajectories. X marks show places where the ionization of the beam occurs.

Figure 2

Experimental setup of HIBP in JIPPT-llU tokamak. Maximum beam energy is 500keV. The radius of a cylindrical deflector is 40cm. An energy analyzer can be adjusted in horizontal and vertical directions with fixed point at the input slit. The voltage of upper electrode in the analyzer is 100kV when beam energy is 500keV. The ripple of the accelerating voltage is less than 2 volts.

Figure 3

The beam trajectory of HIBP in JIPPT-llU, Toroidal field at r= 93cm is 3 Tesla. Beam Energy is 350keV. Initial v_ϕ at the injection into tokamak is zero. (a) Cross-sectional view. (b) Horizontal view.

Figure 4

Signals of the secondary beam at the split-input slits and at the detector by the D_2 gas puffing. The analyzer voltage is tuned to the doubly ionized particles. Beam energy is 200keV. 2.5 Tesla. Injected Tl^+ beam current is a few μA. (a) General characteristics of the signals at the split slit(up, down, right and left) and at the detectors. The slit structure of the analyzer is also shown. (b) Expanded view of the time behaviours of the slit signals.

(c) Detector currents with different gas puff rate. The upper figure corresponds to gas puff rate of 1.2×10^{-3} torr/50msec. In lower figure, the gas puff rate is 0.8×10^{-3} torr/50msec.

Figure 5

schematics of the trajectories of the primary and secondary beam affected by complex changes of charge state. X mark shows the point where ionization or recombination of the beam occurs. 5a, the trajectory of a recombined secondary beam to the analyzer slit. 5b, the expansion of the primary beam due to recombination and ionization of primary beam, and the trajectory of doubly ionized particles with different entrance angles to the slit due to multiple ionization and recombination process.

Figure 6

A contour of the ratio of toroidal velocity v_ϕ to total beam velocity, v_ϕ / v_b at the analyzer in the plane of poloidal and toroidal(horizontal) sweep angles at the injection into the tokamak JIPP T-IIU. The sweep point is shown in Figure 3a and parameters are the same as those of Figure 3.

Table 1

Cross-sections of thallium at 200keV and 400keV for electron stripping and capture in the hydrogen gas from I.Alvarez and C.Cisneros, Phys.Rev.,**13** 1728 (1976).

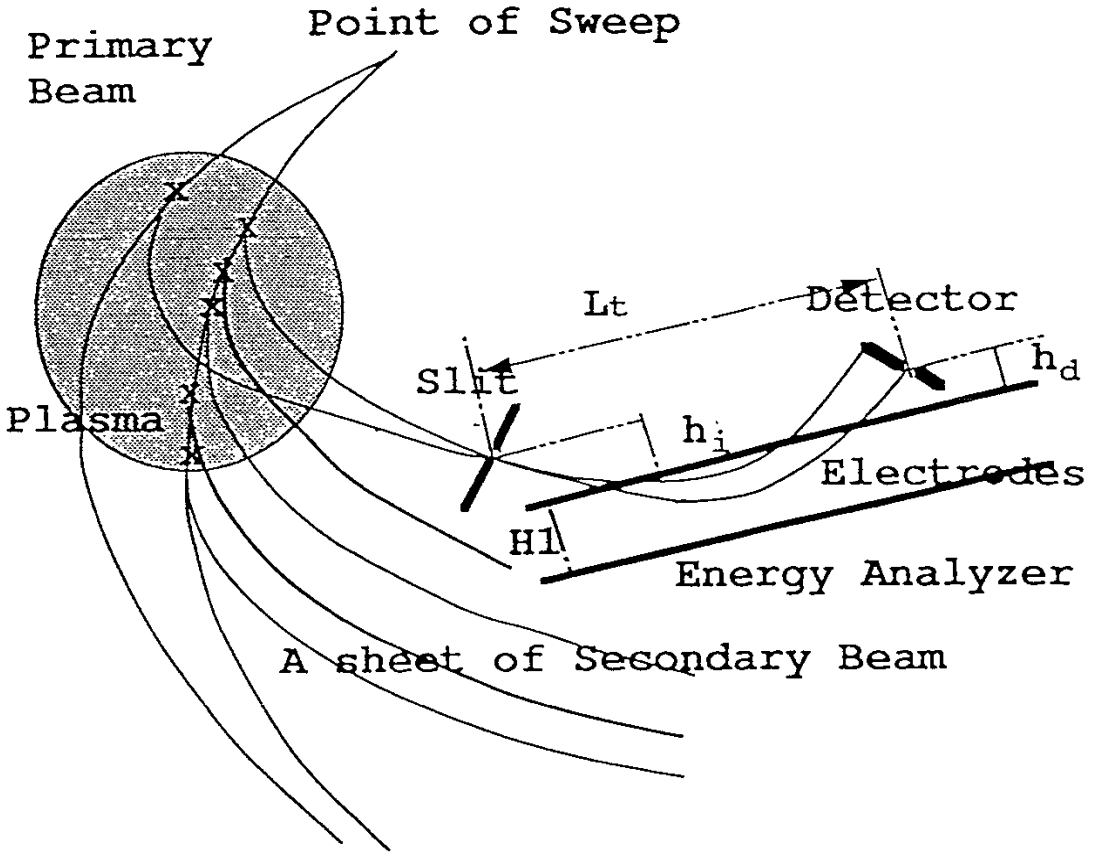
Primary
Beam
Point of Sweep
Plasma
Lt
Detector
Slit
h_d
h_i
Electrodes
H1
Energy Analyzer
A sheet of Secondary Beam

(a)

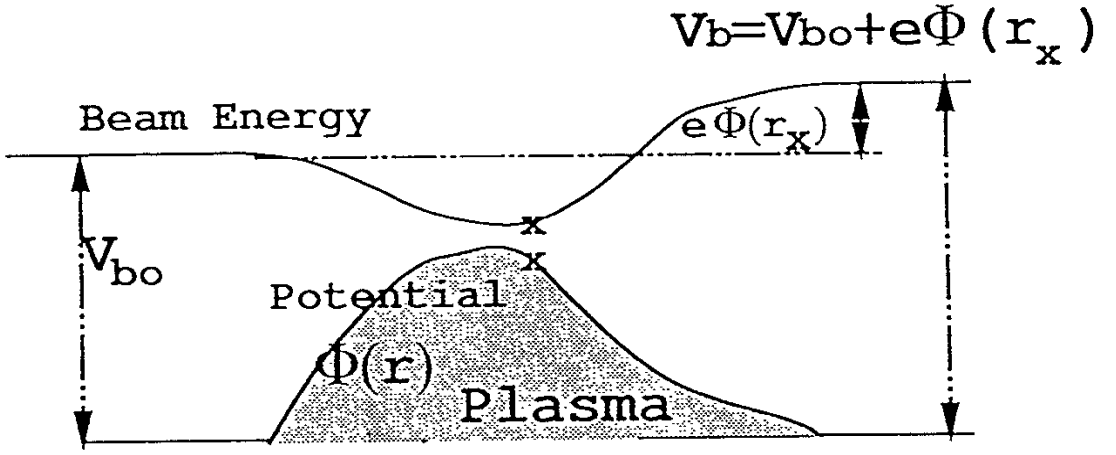
$V_b=V_{bo}+e\Phi(r_x)$
Beam Energy
$e\Phi(r_x)$
V_{bo}
Potential
$\Phi(r)$
Plasma

(b)

Figure 1

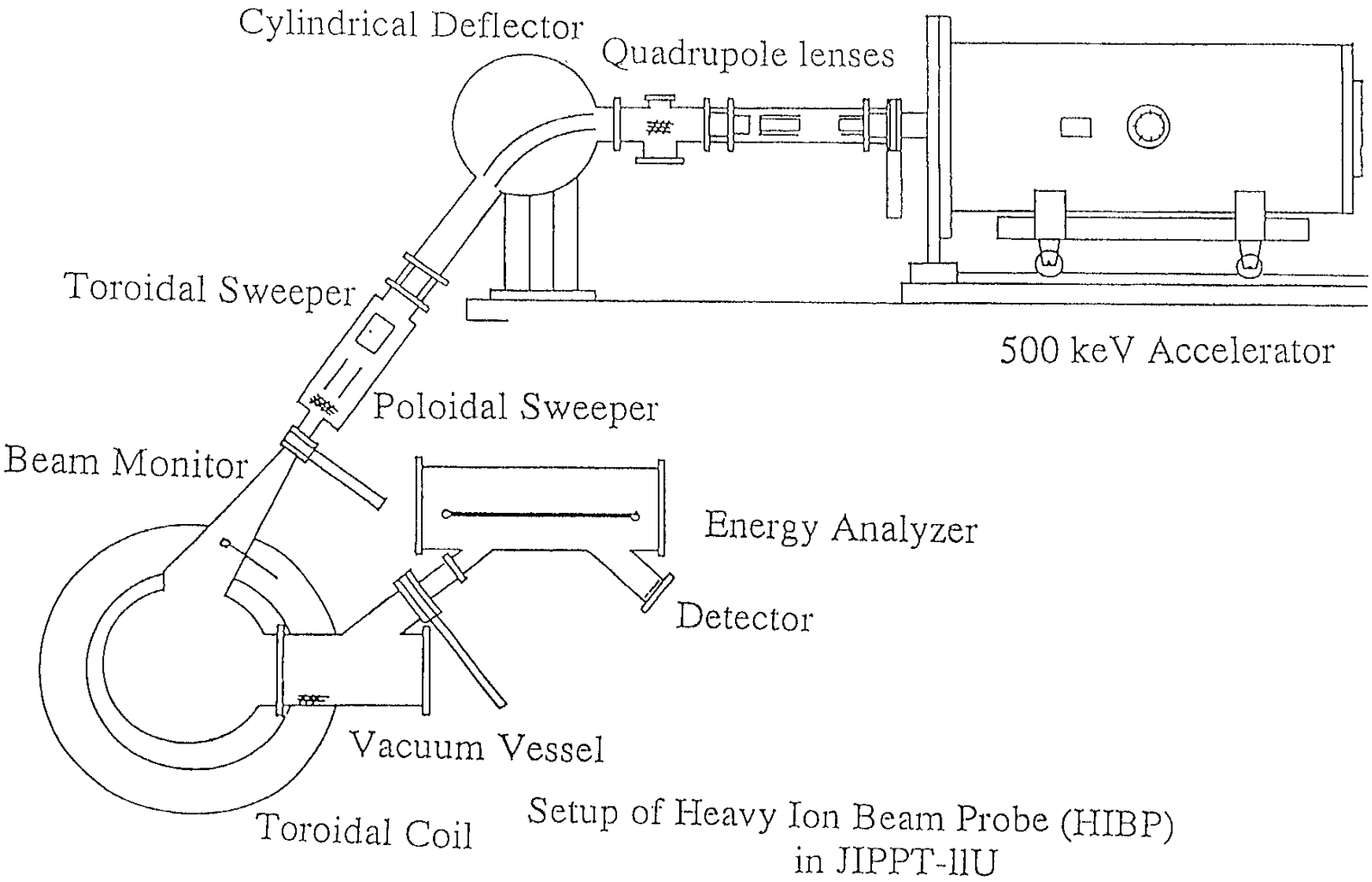
Cylindrical Deflector
Quadrupole lenses
Toroidal Sweeper
500 keV Accelerator
Poloidal Sweeper
Beam Monitor
Energy Analyzer
Detector
Vacuum Vessel
Toroidal Coil
Setup of Heavy Ion Beam Probe (HIBP)
in JIPPT-IIU

Figure 2

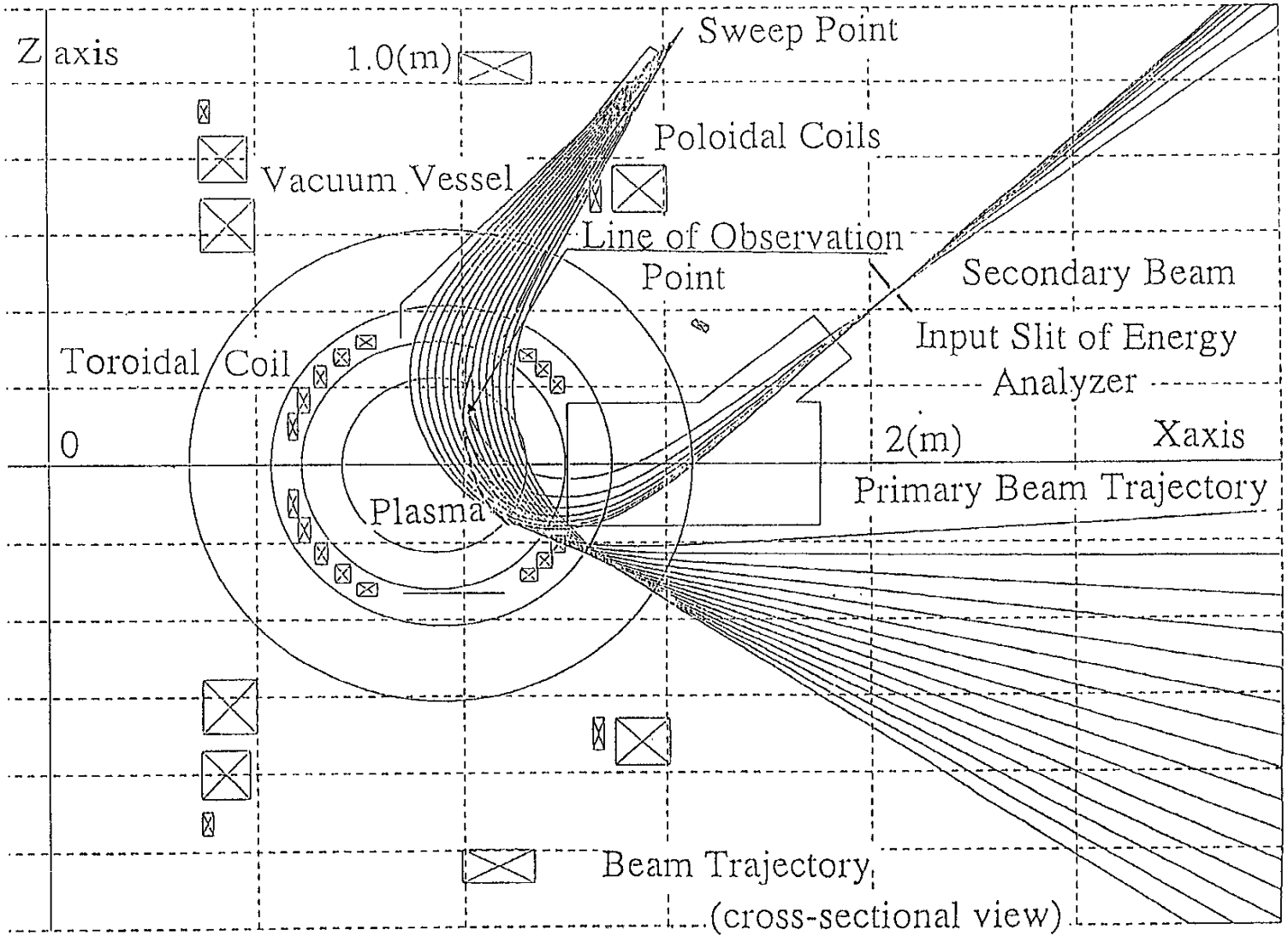
Z axis
1.0(m)
Sweep Point
Poloidal Coils
Vacuum Vessel
Line of Observation
Point
Secondary Beam
Toroidal Coil
Input Slit of Energy
Analyzer
0
2(m)
Xaxis
Primary Beam Trajectory
Plasma
Beam Trajectory
(cross-sectional view)

Figure 3(a)

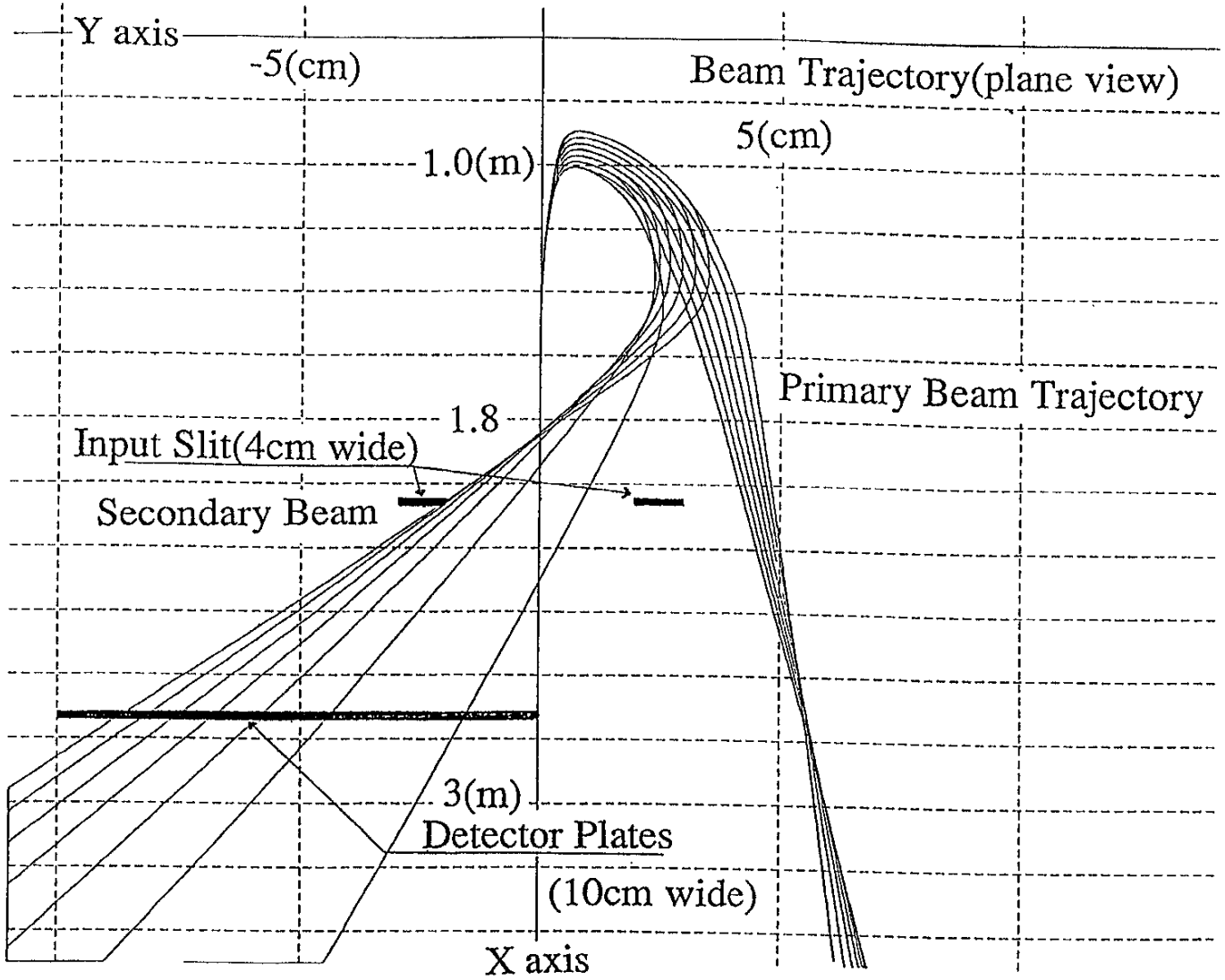
Y axis
-5(cm)
Beam Trajectory(plane view)
5(cm)
1.0(m)
Primary Beam Trajectory
1.8
Input Slit(4cm wide)
Secondary Beam
3(m)
Detector Plates
(10cm wide)
X axis

Figure 3(b)

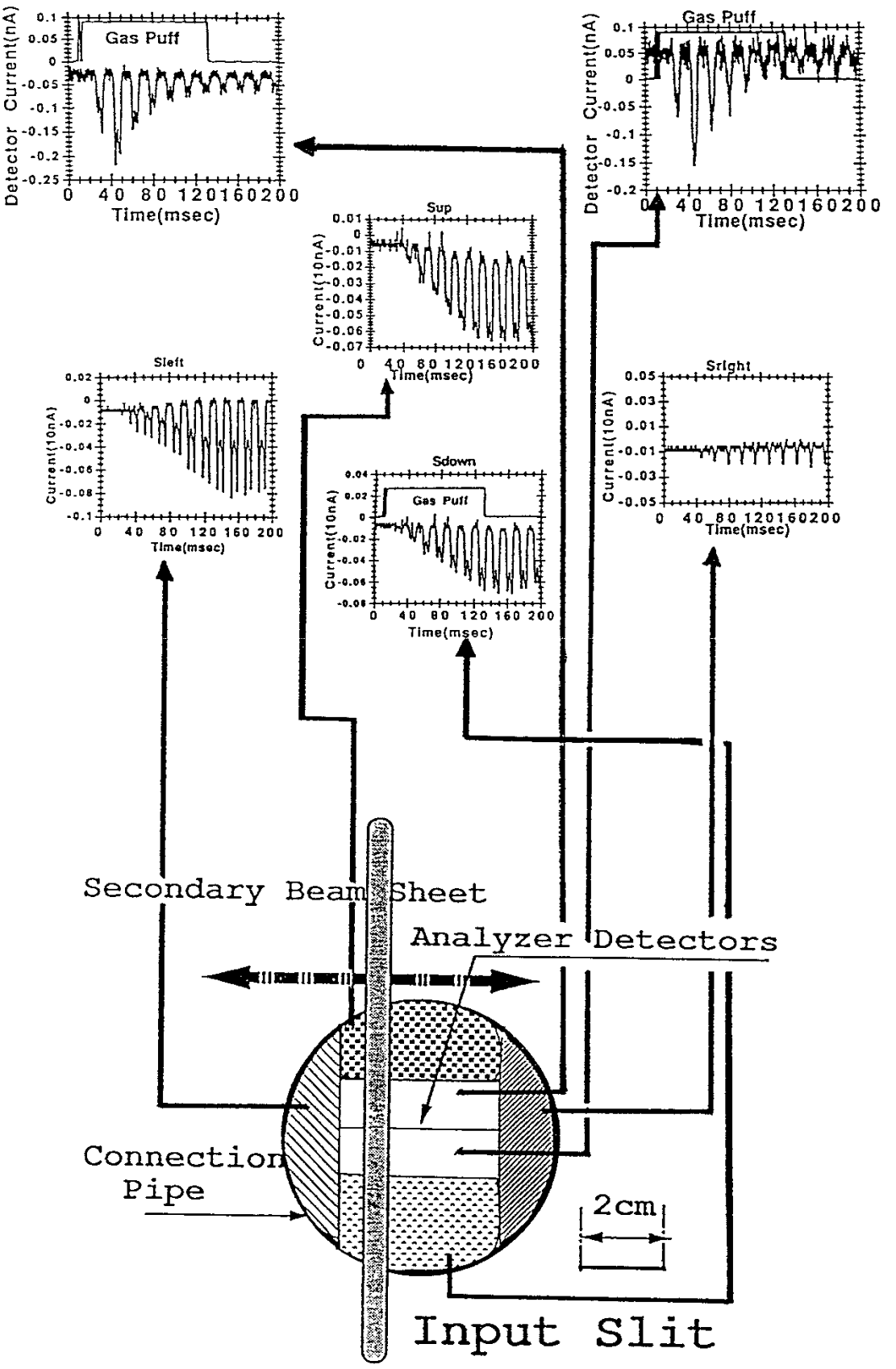
Gas Puff
Detector Current(nA)
Time(msec)
Gas Puff
Detector Current(nA)
Time(msec)
Sup
Current(10nA)
Time(msec)
Sleft
Current(10nA)
Time(msec)
Sright
Current(10nA)
Time(msec)
Sdown
Gas Puff
Current(10nA)
Time(msec)
Secondary Beam Sheet
Analyzer Detectors
Connection
Pipe
2cm
Input Slit

Figure 4(a)

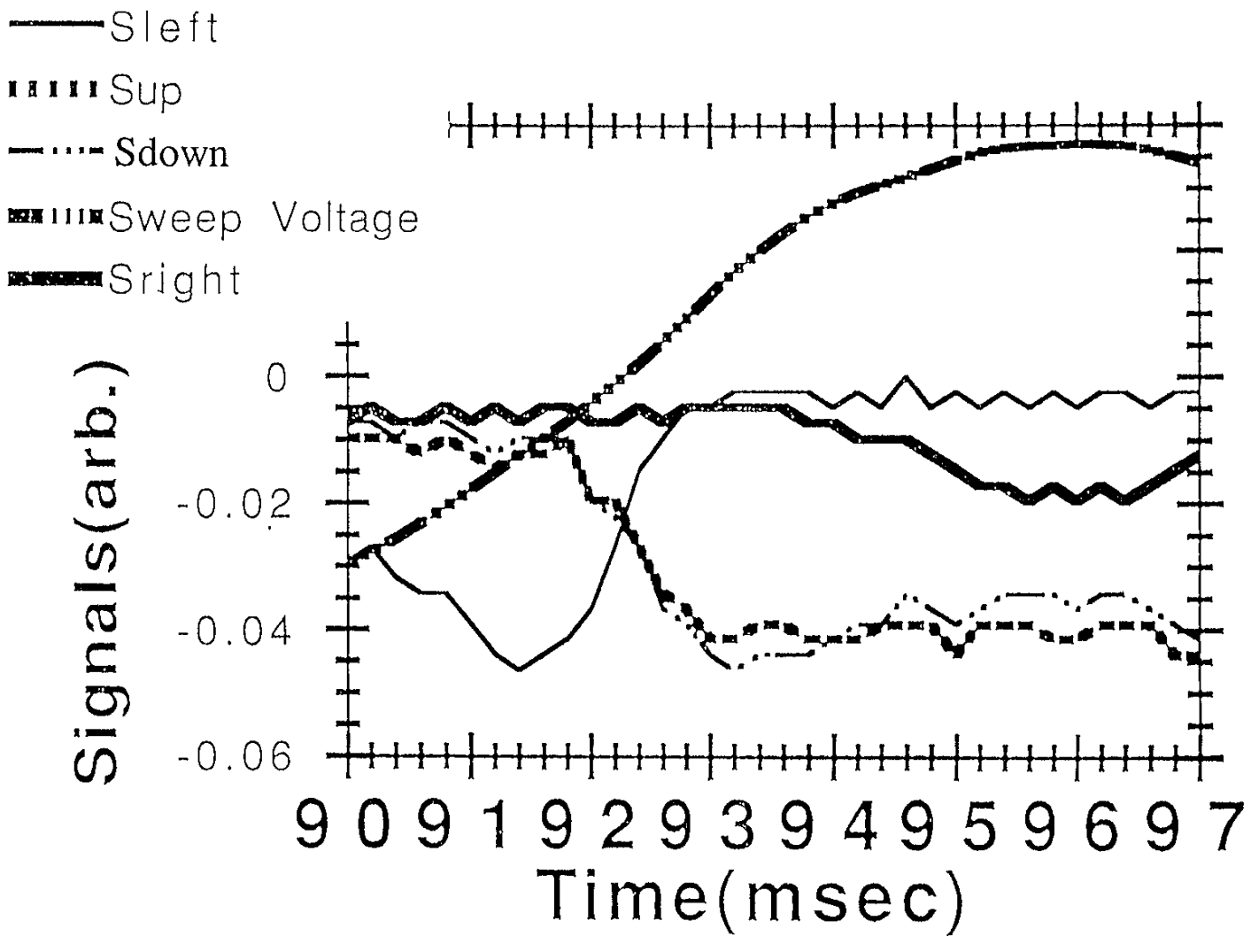
Sleft
Sup
Sdown
Sweep Voltage
Sright
Signals(arb.)
0
-0.02
-0.04
-0.06
90 91 92 93 94 95 96 97
Time(msec)

Figure 4(b)

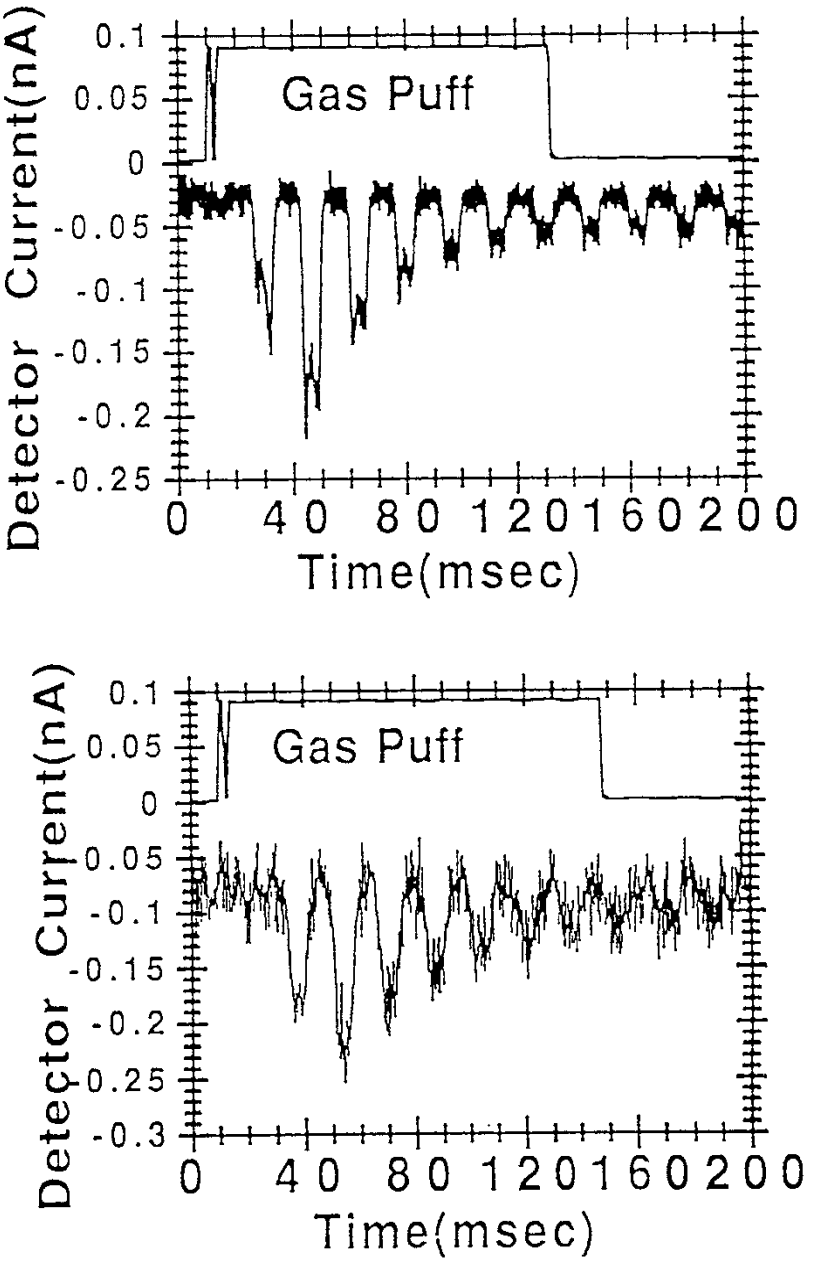
Gas Puff
Detector Current(nA)
0.1
0.05
0
-0.05
-0.1
-0.15
-0.2
-0.25
0 40 80 120 160 200
Time(msec)
Gas Puff
Detector Current(nA)
0.1
0.05
0
0.05
-0.1
-0.15
-0.2
0.25
-0.3
0 40 80 120 160 200
Time(msec)

Figure 4(c)

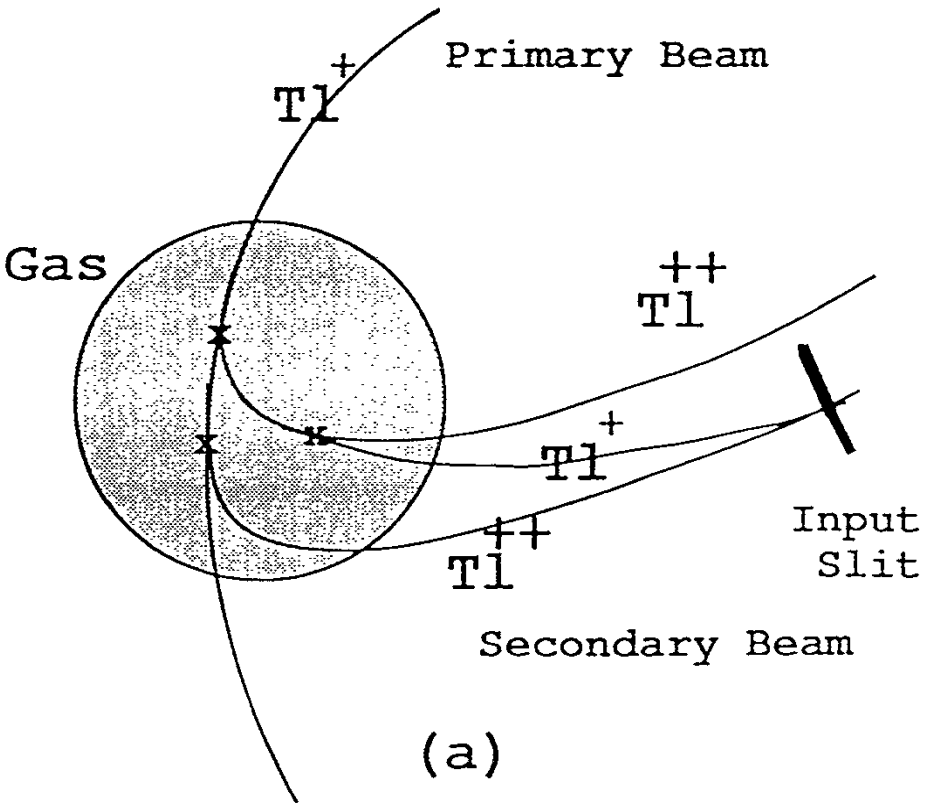
Primary Beam
Tl+
Gas
Tl++
Tl+
Tl++
Input
Slit
Secondary Beam

(a)

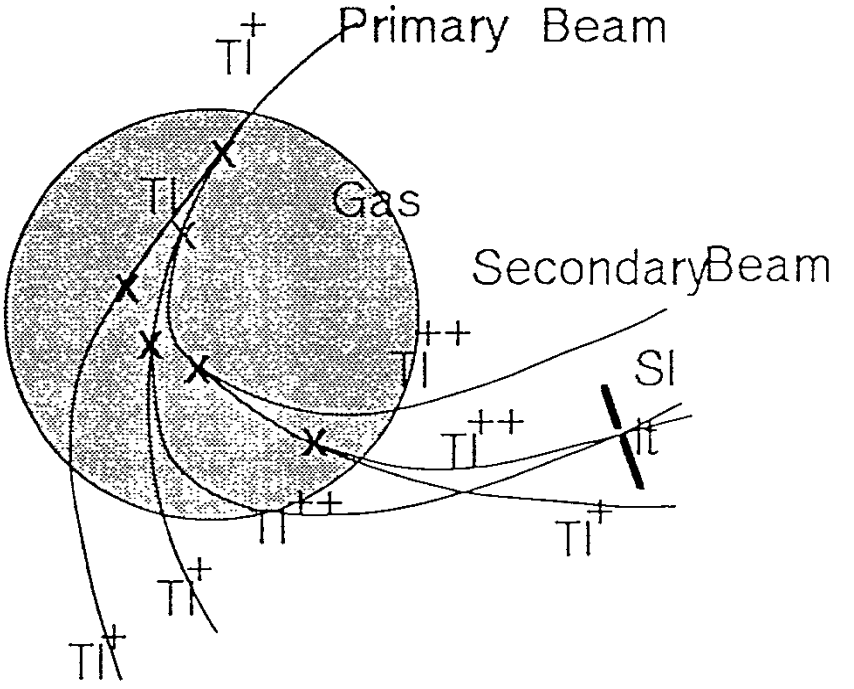
Tl+
Primary Beam
Tl
Gas
Secondary Beam
Tl++
Sl
Tl++
Tl++
Tl+
Tl+
Tl+

(b)

Figure 5

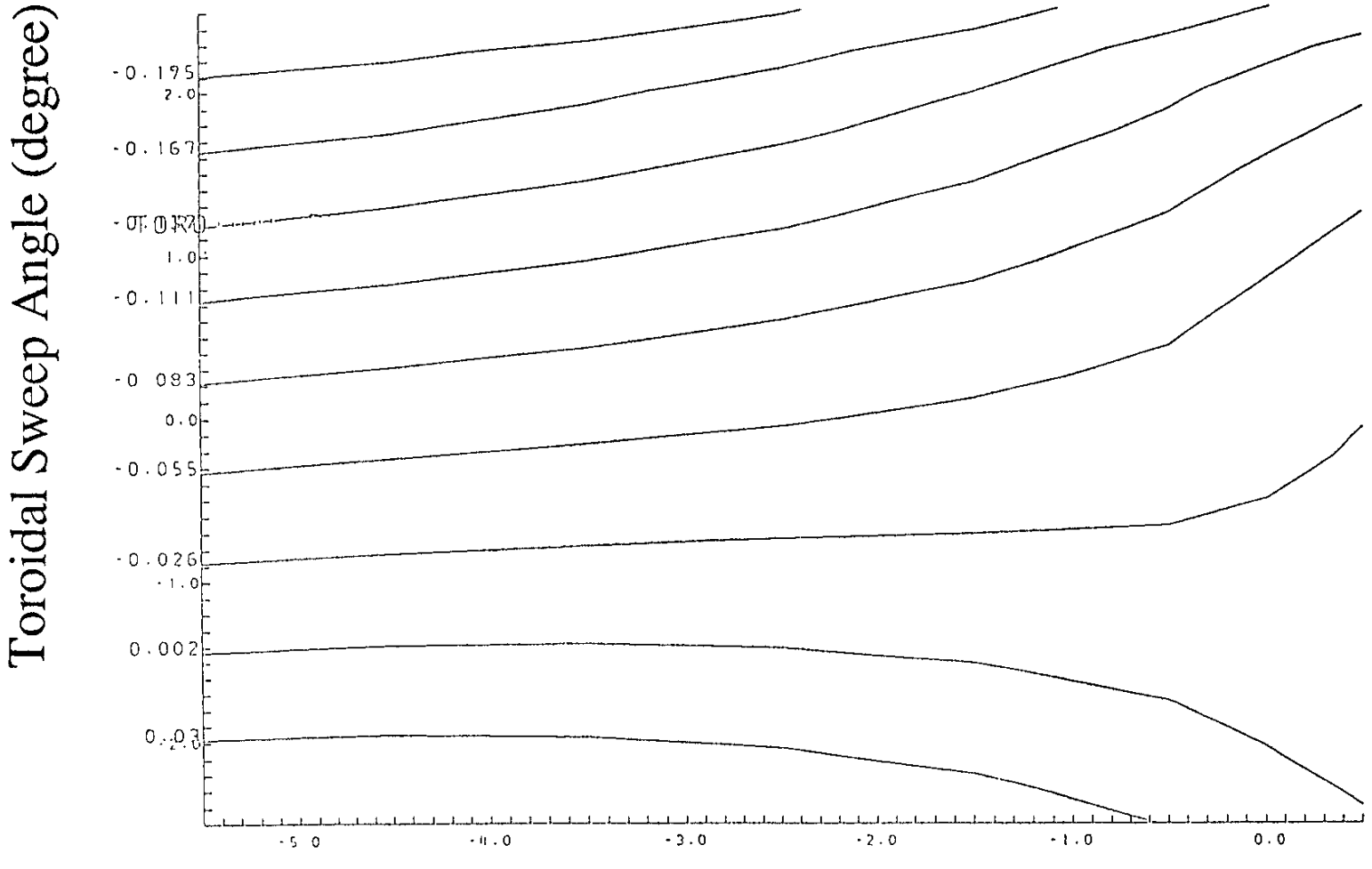
Toroidal Sweep Angle (degree)
-0.195
2.0
-0.167
-0.139
1.0
-0.111
-0.083
0.0
-0.055
-0.026
-1.0
0.002
0.030
-2.0
-5.0
-4.0
-3.0
-2.0
-1.0
0.0
Poloidal Sweep Angle (degree)

Figure 6

Energy (keV) / Reaction	200	400
σ_{10} (10^{-17} cm^3)	4.8	5.1
σ_{01} (10^{-16} cm^3)	4.3	6.3
σ_{12} (10^{-17} cm^3)	1.2	5.1

Table 1

Recent Issues of NIFS Series

NIFS-92 S. - I. Itoh, *H-mode Physics, -Experimental Observations and Model Theories-, Lecture Notes, Spring College on Plasma Physics, May 27 - June 21 1991 at International Centre for Theoretical Physics (IAEA UNESCO) Trieste, Italy ;* Jun. 1991

NIFS-93 Y. Miura, K. Itoh, S. - I. Itoh, T. Takizuka, H. Tamai, T. Matsuda, N. Suzuki, M. Mori, H. Maeda and O. Kardaun, *Geometric Dependence of the Scaling Law on the Energy Confinement Time in H-mode Discharges;* Jun. 1991

NIFS-94 H. Sanuki, K. Itoh, K. Ida and S. - I. Itoh, *On Radial Electric Field Structure in CHS Torsatron / Heliotron;* Jun. 1991

NIFS-95 K. Itoh, H. Sanuki and S. - I. Itoh, *Influence of Fast Ion Loss on Radial Electric Field in Wendelstein VII-A Stellarator;* Jun. 1991

NIFS-96 S. - I. Itoh, K. Itoh, A. Fukuyama, *ELMy-H mode as Limit Cycle and Chaotic Oscillations in Tokamak Plasmas;* Jun. 1991

NIFS-97 K. Itoh, S. - I. Itoh, H. Sanuki, A. Fukuyama, *An H-mode-Like Bifurcation in Core Plasma of Stellarators;* Jun. 1991

NIFS-98 H. Hojo, T. Watanabe, M. Inutake, M. Ichimura and S. Miyoshi, *Axial Pressure Profile Effects on Flute Interchange Stability in the Tandem Mirror GAMMA 10;* Jun. 1991

NIFS-99 A. Usadi, A. Kageyama, K. Watanabe and T. Sato, *A Global Simulation of the Magnetosphere with a Long Tail : Southward and Northward IMF;* Jun. 1991

NIFS-100 H. Hojo, T. Ogawa and M. Kono, *Fluid Description of Ponderomotive Force Compatible with the Kinetic One in a Warm Plasma* ; July 1991

NIFS-101 H. Momota, A. Ishida, Y. Kohzaki, G. H. Miley, S. Ohi, M. Ohnishi K. Yoshikawa, K. Sato, L. C. Steinhauer, Y. Tomita and M. Tuszewski *Conceptual Design of D-^{3}He FRC Reactor "ARTEMIS"* ; July 1991

NIFS-102 N. Nakajima and M. Okamoto, *Rotations of Bulk Ions and Impurities in Non-Axisymmetric Toroidal Systems* ; July 1991

NIFS-103 A. J. Lichtenberg, K. Itoh, S. - I. Itoh and A. Fukuyama, *The Role of Stochasticity in Sawtooth Oscillation* ; Aug. 1991

NIFS-104 K. Yamazaki and T. Amano, *Plasma Transport Simulation Modeling for Helical Confinement Systems;* Aug. 1991

NIFS-105 T. Sato, T. Hayashi, K. Watanabe, R. Horiuchi, M. Tanaka, N. Sawairi and K. Kusano, *Role of Compressibility on Driven Magnetic Reconnection ;* Aug. 1991

NIFS-106 Qian Wen - Jia, Duan Yun - Bo, Wang Rong - Long and H. Narumi, *Electron Impact Excitation of Positive Ions - Partial Wave Approach in Coulomb - Eikonal Approximation* ; Sep. 1991

NIFS-107 S. Murakami and T. Sato, *Macroscale Particle Simulation of Externally Driven Magnetic Reconnection;* Sep. 1991

NIFS-108 Y. Ogawa, T. Amano, N. Nakajima, Y. Ohyabu, K. Yamazaki, S. P. Hirshman, W. I. van Rij and K. C. Shaing, *Neoclassical Transport Analysis in the Banana Regime on Large Helical Device (LHD) with the DKES Code;* Sep. 1991

NIFS-109 Y. Kondoh, *Thought Analysis on Relaxation and General Principle to Find Relaxed State;* Sep. 1991

NIFS-110 H. Yamada, K. Ida, H. Iguchi, K. Hanatani, S. Morita, O. Kaneko, H. C. Howe, S. P. Hirshman, D. K. Lee, H. Arimoto, M. Hosokawa, H. Idei, S. Kubo, K. Matsuoka, K. Nishimura, S. Okamura, Y. Takeiri, Y. Takita and C. Takahashi, *Shafranov Shift in Low-Aspect-Ratio Heliotron / Torsatron CHS* ; Sep 1991

NIFS-111 R. Horiuchi, M. Uchida and T. Sato, *Simulation Study of Stepwise Relaxation in a Spheromak Plasma ;* Oct. 1991

NIFS-112 M. Sasao, Y. Okabe, A. Fujisawa, H. Iguchi, J. Fujita, H. Yamaoka and M. Wada, *Development of Negative Heavy Ion Sources for Plasma Potential Measurement* ; Oct. 1991

NIFS-113 S. Kawata and H. Nakashima, *Tritium Content of a DT Pellet in Inertial Confinement Fusion* ; Oct. 1991

NIFS-114 M. Okamoto, N. Nakajima and H. Sugama, *Plasma Parameter Estimations for the Large Helical Device Based on the Gyro-Reduced Bohm Scaling* ; Oct. 1991

NIFS-115 Y. Okabe, *Study of Au^- Production in a Plasma-Sputter Type Negative Ion Source* ; Oct. 1991

NIFS-116 M. Sakamoto, K. N. Sato, Y. Ogawa, K. Kawahata, S. Hirokura, S. Okajima, K. Adati, Y. Hamada, S. Hidekuma, K. Ida, Y. Kawasumi, M. Kojima, K. Masai, S. Morita, H. Takahashi, Y. Taniguchi, K. Toi and

T. Tsuzuki, *Fast Cooling Phenomena with Ice Pellet Injection in the JIPP T-IIU Tokamak;* Oct. 1991

NIFS-117 K. Itoh, H. Sanuki and S. -I. Itoh, *Fast Ion Loss and Radial Electric Field in Wendelstein VII-Λ Stellarator*; Oct. 1991

NIFS-118 Y. Kondoh and Y. Hosaka, *Kernel Optimum Nearly-analytical Discretization (KOND) Method Applied to Parabolic Equations <<KOND-P Scheme>>;* Nov. 1991

NIFS-119 T. Yabe and T. Ishikawa, *Two- and Three-Dimensional Simulation Code for Radiation-Hydrodynamics in ICF*; Nov. 1991

NIFS-120 S. Kawata, M. Shiromoto and T. Teramoto, *Density-Carrying Particle Method for Fluid* ; Nov. 1991

NIFS-121 T. Ishikawa, P. Y. Wang, K. Wakui and T. Yabe, *A Method for the High-speed Generation of Random Numbers with Arbitrary Distributions;* Nov. 1991

NIFS-122 K. Yamazaki, H. Kaneko, Y. Taniguchi, O. Motojima and LHD Design *Group, Status of LHD Control System Design ; Dec. 1991*

NIFS-123 Y. Kondoh, *Relaxed State of Energy in Incompressible Fluid and Incompressible MHD Fluid* ; Dec. 1991

NIFS-124 K. Ida, S. Hidekuma, M. Kojima, Y. Miura, S. Tsuji, K. Hoshino, M. Mori, N. Suzuki, T. Yamauchi and JFT-2M Group, *Edge Poloidal Rotation Profiles of H-Mode Plasmas in the JFT-2M Tokamak ;* Dec. 1991

NIFS-125 H. Sugama and M. Wakatani, *Statistical Analysis of Anomalous Transport in Resistive Interchange Turbulence* ;Dec. 1991

NIFS-126 K. Narihara, *A Steady State Tokamak Operation by Use of Magnetic Monopoles* ; Dec. 1991

NIFS-127 K. Itoh, S. -I. Itoh and A. Fukuyama, *Energy Transport in the Steady State Plasma Sustained by DC Helicity Current Drive* ;Jan. 1992

NIFS-128 Y. Hamada, Y. Kawasumi, K. Masai, H. Iguchi, A. Fujisawa, JIPP T-IIU Group and Y. Abe, *New Hight Voltage Parallel Plate Analyzer* ; Jan. 1992

NIFS-129 K. Ida and T. Kato, *Line-Emission Cross Sections for the Charge-exchange Reaction between Fully Stripped Carbon and Atomic Hydrogen in Tokamak*

Plasma; Jan. 1992

NIFS-130 T. Hayashi, A. Takei and T. Sato, *Magnetic Surface Breaking in 3D MHD Equilibria of l=2 Heliotron* ; Jan. 1992

NIFS-131 K. Itoh, K. Ichiguchi and S. -I. Itoh, *Beta Limit of Resistive Plasma in Torsatron/Heliotron* ; Feb. 1992

NIFS-132 K. Sato and F. Miyawaki, *Formation of Presheath and Current-Free Double Layer in a Two-Electron-Temperature Plasma* ; Feb. 1992

NIFS-133 T. Maruyama and S. Kawata, *Superposed-Laser Electron Acceleration* Feb. 1992

NIFS-134 Y. Miura, F. Okano, N. Suzuki, M. Mori, K. Hoshino, H. Maeda, T. Takizuka, JFT-2M Group, S.-I. Itoh and K. Itoh, *Rapid Change of Hydrogen Neutral Energy Distribution at L/H-Transition in JFT-2M H-mode ;* Feb. 1992

NIFS-135 H. Ji, H. Toyama, A. Fujisawa, S. Shinohara and K. Miyamoto *Fluctuation and Edge Current Sustainment in a Reversed-Field-Pinch;* Feb. 1992

NIFS-136 K. Sato and F. Miyawaki, *Heat Flow of a Two-Electron-Temperature Plasma through the Sheath in the Presence of Electron Emission;* Mar. 1992

NIFS-137 T. Hayashi, U. Schwenn and E. Strumberger, *Field Line Diversion Properties of Finite ß Helias Equilibria;* Mar. 1992

NIFS-138 T. Yamagishi, *Kinetic Approach to Long Wave Length Modes in Rotating Plasmas*; Mar.. 1992

NIFS-139 K. Watanabe, N. Nakajima, M. Okamoto, Y. Nakamura and M. Wakatani, *Three-dimensional MHD Equilibrium in the Presence of Bootstrap Current for Large Helical Device (LHD)*; Mar. 1992

NIFS-140 K. Itoh, S. -I. Itoh and A. Fukuyama, *Theory of Anomalous Transport in Toroidal Helical Plasmas;* Mar. 1992

NIFS-141 Y. Kondoh, *Internal Structures of Self-Organized Relaxed States and Self-Similar Decay Phase;* Mar. 1992

NIFS-142 U. Furukane, K. Sato, K. Takiyama and T. Oda, *Recombining Processes in a Cooling Plasma by Mixing of Initially Heated Gas*; Mar. 1992